Self-Assembly of Single-Walled Carbon Nanotubes into Multiwalled Carbon Nanotubes in Water: Molecular Dynamics Simulations

ARTICLE *in* NANO LETTERS · APRIL 2006

Impact Factor: 13.59 · DOI: 10.1021/nl052289u · Source: PubMed

4 AUTHORS, INCLUDING:

Xi-Qiao Feng
Tsinghua University
329 PUBLICATIONS **5,478** CITATIONS

SEE PROFILE

Huajian Gao
Brown University
553 PUBLICATIONS **22,802** CITATIONS

SEE PROFILE

NANO LETTERS

2006
Vol. 6, No. 3
430−434

Self-Assembly of Single-Walled Carbon Nanotubes into Multiwalled Carbon Nanotubes in Water: Molecular Dynamics Simulations

Jian Zou,[†] Baohua Ji,[†] Xi-Qiao Feng,[†] and Huajian Gao*[,‡]

Department of Engineering Mechanics, Tsinghua University, Beijing 100084, China, and Max Planck Institute for Metals Research, Heisenbergstrasse 3, D-70569 Stuttgart, Germany

Received November 19, 2005; Revised Manuscript Received January 2, 2006

ABSTRACT

We report discoveries from a series of molecular dynamics simulations that single-walled carbon nanotubes, with different diameters, lengths, and chiralities, can coaxially self-assemble into multiwalled carbon nanotubes in water via spontaneous insertion of smaller tubes into larger ones. The assembly process is tube-size-dependent, and the driving force is primarily the intertube van der Waals interactions. The simulations also suggest that a multiwalled carbon nanotube may be separated into single-walled carbon nanotubes under appropriate solvent conditions. This study suggests possible bottom-up self-assembly routes for the fabrication of novel nanodevices and systems.

The extraordinary physical, chemical, and mechanical properties[1,2] of carbon nanotubes (CNTs) have made them attractive materials for numerous applications.[3,4] A multiwalled carbon nanotube (MWNT) consists of concentrically nested shells of single-walled carbon nanotubes (SWNTs) of different diameters.[5] As suggested by Drexler,[6] such multilayer structures may be fabricated by consecutively inserting smaller shells into larger ones. The atomically smooth tube surfaces of MWNTs allow nearly frictionless intershell sliding and rotation with a very short reaction time.[7−11] These fascinating properties suggest that MWNTs hold great potential in building robust and efficient nanomachines in future nanoelectromechanical systems (NEMS), for example, nanobearings,[7−9] oscillators,[10−12] nanorotors,[13,14] and numerous other devices.[15−17]

The fast development in fullerene engineering and nanotechnology is stimulated by, among other reasons, the desire to shrink the size of integrated circuits as well as to assemble structures and devices at the nanoscale level.[3,4,18] At this scale, physical manipulation poses great challenges on positioning, fabricating, and assembling machines and devices as well as driving their motions in a controllable manner.[10] To date, these manipulation techniques are still hardly achievable or far from routine for practical applications.

In this letter, we report discoveries from molecular dynamics (MD) simulations that SWNTs, with different diameters, lengths, and chiralities, can coaxially self-assemble into MWNTs in a water solution. This spontaneous assembly process in water is driven primarily by the vdW interaction between nanotubes of different sizes. Our results suggest a promising "bottom-up" approach for building MWNTs from SWNTs with desired structures or properties for specific applications in NEMS. For example, a double-walled CNT might be formed by inserting a metallic CNT into an insulating one like a coaxial wire. MWNT-based nanostructures fabricated in this manner may be used as starting materials for more complex machines or devices in NEMS.

Because the CNT−water system is expected to be nonhomogeneous at the atomic scale due to layered water structures in the vicinity of CNTs,[19] molecular dynamics simulations using GROMACS[20,21] are selected as the tool to study the coaxial self-assembly of CNTs in an orthorhombic water box at the room temperature of 300 K and atmospheric pressure of 1 bar.[22] The CNTs are described by a Morse bond, a harmonic cosine bending angle,

* Corresponding author. E-mail: hjgao@mf.mpg.de.
[†] Department of Engineering Mechanics, Tsinghua University.
[‡] Max Planck Institute for Metals Research, Heisenbergstrasse 3, D-70569 Stuttgart, Germany. Present Address: Division of Engineering, Brown University, 182 Hope Street, Providence, RI 02912.

10.1021/nl052289u CCC: $33.50
Published on Web 01/26/2006

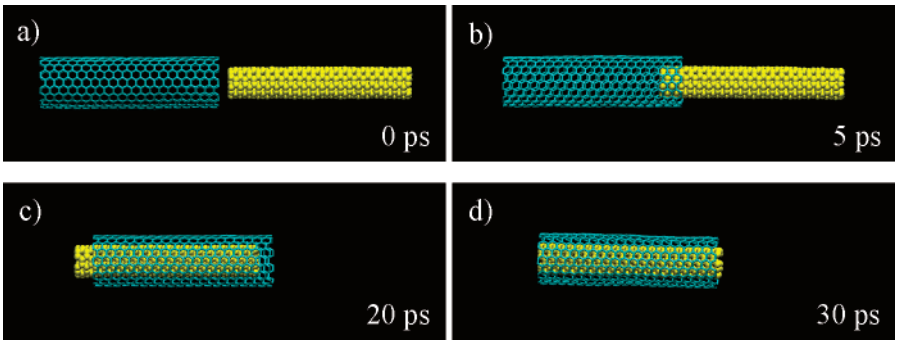

Figure 1. Simulation snapshots of the self-assembly process of a (5,5) nanotube entering a (10,10) nanotube at $t = 0$, 5, 20, and 30 ps, respectively. The two CNTs have the same length of 4.79 nm. Water molecules are not displayed for clarity.

Table 1. Parameters for Interaction Potentials Used in the Simulations[a]

$K_{Cr} = 478.9$ kJ mol^{-1}	$r_C = 0.1418$ nm, $\gamma = 21.867$ nm^{-1}
$K_{C\theta} = 562.2$ kJ mol^{-1}	$\theta_C = 120^0$
$K_{C\phi} = 25.12$ kJ mol^{-1}	$\phi_C = 180^0$
$\epsilon_{CC} = 0.3601$ kJ mol^{-1}	$\sigma_{CC} = 0.3400$ nm
$\epsilon_{CO} = 0.4787$ kJ mol^{-1}	$\sigma_{CO} = 0.3275$ nm

[a] The bonding parameters for CNTs are taken from ref 19 (K_{Cr}, r_C, and γ are the parameters for the Morse bond potential; $K_{C\theta}$, and θ_C are the parameters for the bending angle potential; $K_{C\phi}$, and ϕ_C are the torsion parameters) and the nonbonding parameters from ref 26 (ϵ_{CC} and σ_{CC} are the Lennard−Jones parameters for carbon−carbon interactions; ϵ_{CO} and σ_{CO} are the Lennard−Jones parameters for carbon−oxygen interactions). Carbon atoms are treated as uncharged particles. The TIP3P model[23] is used to describe water molecules with partial charges assigned to oxygen and hydrogen atoms.

a twofold cosine torsion, and a Lennard−Jones (LJ) 12−6 term as[19]

$$U(r_{ij},\theta_{ijk},\phi_{ijkl}) = K_{Cr}[e^{-\gamma(r_{ij}-r_C)} - 1]^2 + \frac{1}{2}K_{C\theta}(\cos\theta_{ijk} - \cos\theta_C)^2 + \frac{1}{2}K_{C\phi}(1 - \cos 2\phi_{ijkl}) + 4\epsilon_{CC}\left[\left(\frac{\sigma_{CC}}{r_{ij}}\right)^{12} - \left(\frac{\sigma_{CC}}{r_{ij}}\right)^{6}\right] \quad (1)$$

The water solvent is modeled by the transferable intermolecular potential three-point (TIP3P) model,[23] and the electrostatic interactions are evaluated by the particle mesh Ewald (PME) method.[24,25] The CNT−water interaction is described by a carbon−oxygen LJ potential.[26] For conciseness and clarity, all of the parameters involved are summarized in Table 1. In our simulations, the CNTs are initially aligned coaxially, as shown in Figure 1a, and the distance between the ends of the two CNTs is set to be 0.2 nm. No position restraint is applied on CNTs so that they are free to have both translational and rotational motions.

We start with the simulation of coaxial assembly of two armchair SWNTs (5,5) and (10,10) having the same length of 4.79 nm. The simulation shows an extremely fast insertion process of the smaller (5,5) tube into the (10,10) tube (see Figure 1). The proximal "head" of the (5,5) begins to enter the (10,10) at $t = 5$ ps, and the full encapsulation of the smaller CNT into the larger one is completed at about $t = 20$ ps. Afterward, the (5,5) CNT oscillates slightly inside the (10,10) because of inertia forces and the intertube van

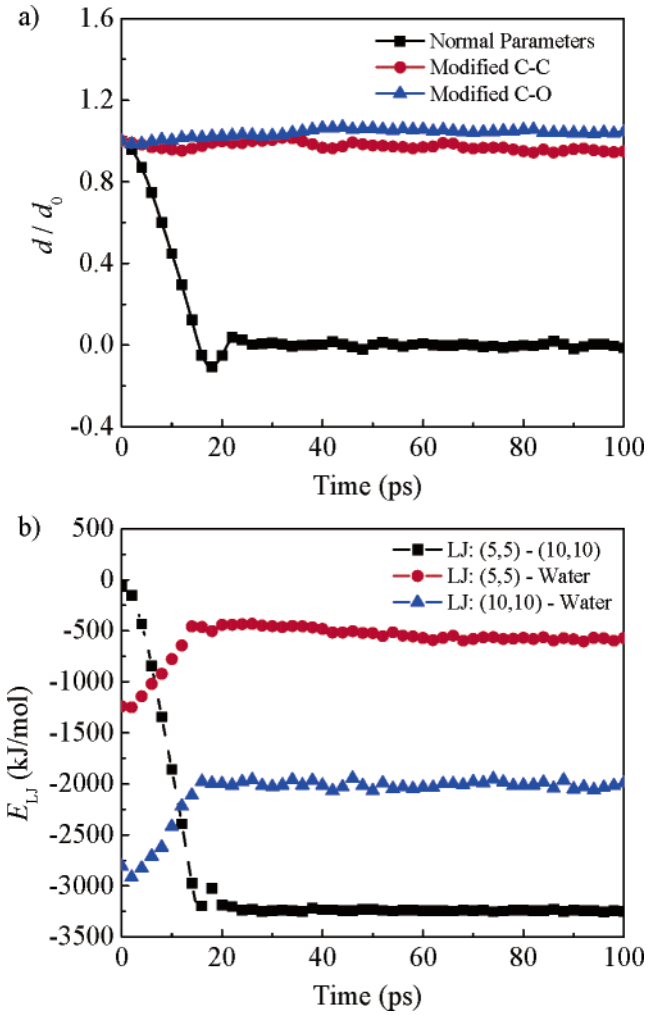

Figure 2. The dynamic assembly process of (5,5) and (10,10) nanotubes. (a) Normalized center-of-mass (COM) distances between the (5,5) and (10,10) nanotubes as a function of time, where d_0 is the initial spacing between the two tubes. For the simulation with normal parameters listed in Table 1, the intertube COM distance decreases rapidly in the first 20 ps (the black curve). The nearly constant $d = 0$ afterward indicates that the assembled system has reached equilibrium. For the simulations using reduced carbon−carbon attraction parameters (the blue curve, with $\sigma_{CC} = 0.3816$ nm and $\epsilon_{CC} = 0.9002$ kJ/mol) or increased carbon−water attraction parameters (the red curve, with $\sigma_{CO} = 0.2918$ nm and $\epsilon_{CO} = 1.9148$ kJ/mol), the intertube COM distance has no apparent change, indicating that the two CNTs could not assemble together. (b) The evolution of van der Waals energy for a CNT−CNT interaction and CNT−water interactions as a function of time, where the parameters listed in Table 1 are adopted.

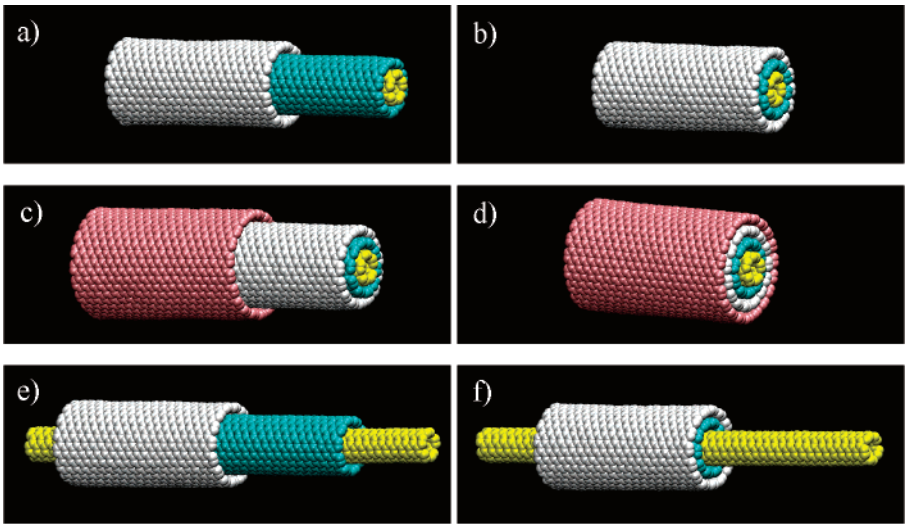

Figure 3. Simulation snapshots of stepwise assembly of SWNTs into MWNTs. (a−b) Snapshots of assembling a double-walled CNT (5,5)@(10,10) into SWNT (15,15) at $t = 10$ ps and $t = 30$ ps. (c−d) Snapshots of assembling a triple-walled CNT (5,5)@(10,10)@(15,15) into SWNT (20,20) at $t = 10$ ps and $t = 30$ ps. (e−f) Snapshots of assembling (5,5), (10,10), and (15, 15) CNTs with different lengths at $t = 10$ ps and $t = 30$ ps.

de Waals attraction. The oscillation is dissipated rapidly within the next 10 ps because of the resistance of the surrounding water molecules. After $t = 30$ ps, the self-assembled double-walled CNT reaches equilibrium. This ultrafast assembly process is confirmed by the change in the center-of-mass (COM) distance between the two CNTs as a function of simulation time (see the black curve in Figure 2a).

To reveal the physical mechanisms of this assembly process, the corresponding vdW energy is plotted in Figure 2b. The CNT−CNT vdW energy between the (5,5) and (10,-10) CNTs decreases rapidly as a function of the insertion time while the vdW energy values of both (5,5)-water and (10,10)-water increase in a slower rate. Therefore, the reduction in the intertube vdW energy suffices to compensate the energy cost to repel water molecules away from the CNTs and serves as the primary driving force for the self-assembly process. The dominant role of vdW interactions in the assembly process can be examined by tuning the strength of vdW interactions. We find that the process of a (5,5) tube entering a (10,10) tube can be stopped by either halving the nonbond carbon−carbon interaction or doubling the carbon−water attraction (as shown by the red and the blue curves in Figure 2a, respectively). This demonstrates that the assembly process is determined by the competition between the intertube vdW attraction and interaction of the CNTs with the surrounding water molecules. Such modifications of vdW attractions may be regarded as mimicking changes in the local polarity of tubes and solvent conditions.[26−28] We also find that a preinserted (5,5) CNT would spring out of a (10,-10) tube when the carbon−water vdW attraction is doubled, thereby disassembling a double-walled CNT into two separate SWNTs. This observation suggests that an MWNT could also be separated into SWNTs when the CNT-solvent attraction is stronger than the CNT−CNT vdW attraction.

Further simulations show that similar assembly processes can occur for other MWNTs (see Figure 3). For instance, we find that a double-walled CNT (5,5)@(10,10) and an SWNT (15,15) placed in water spontaneously assemble into a triple-walled CNT (see Figure 3a and b); the resulting triple-walled CNT and a larger SWNT (20,20) placed into water further assemble into a tetrawalled CNT (see Figure 3c and d). Both processes happen within 30 ps. This consecutive shell-by-shell assembly offers a possible approach to efficiently fabricating an MWNT from a set of given SWNTs via a series of insertion processes as shown above. The CNTs of different sizes can coaxially assemble into a desired MWNT under controllable processing steps. One example of this kind of assembled structure is shown in Figure 3e and f, where the innermost (5,5) CNT is 12.2 nm long, and the other two (10,10) and (15,15) are 4.79 nm long. First, the (10,10) and (15,15) CNTs coaxially assemble onto the (5,5) from its two ends, respectively. Then the (10,-10) and (15,15) are assembled together along the (5,5) CNT, which serves to keep the (10,10) and (15,15) coaxially aligned during the assembly process.

Because the strength of the CNT−CNT vdW interactions depends on the intertube spacing between the CNTs, the assembly process is expected to be strongly tube-size-dependent. To explore this size effect, we designed a set of simulations by varying the diameters of the large SWNT in the system described in Figure 1, and compared the assembly processes of a (5,5) CNT into (9,9), (12,12), (15,15), and (20,20) tubes, respectively. The radii of the small and large CNTs as well as their differences (referred to as ΔR) are listed in Table 2. The vdW energy between the two CNTs in Figure 4a indicates that the slope of the intertube vdW energy with respect to the COM distance decreases with the increase in ΔR. The larger the ΔR, the slower the assembly process (Figure 4b). The insertion speed decreases exponentially with respect to ΔR (Figure 4c). In addition, when ΔR becomes very large, for example, for a combination of (5,5) and (20,20) CNTs, the insertion pathway of the small CNT may depart from the original coaxial trajectory. The small tube will move toward the interior wall of the large tube and thereafter assembles along this interior wall instead

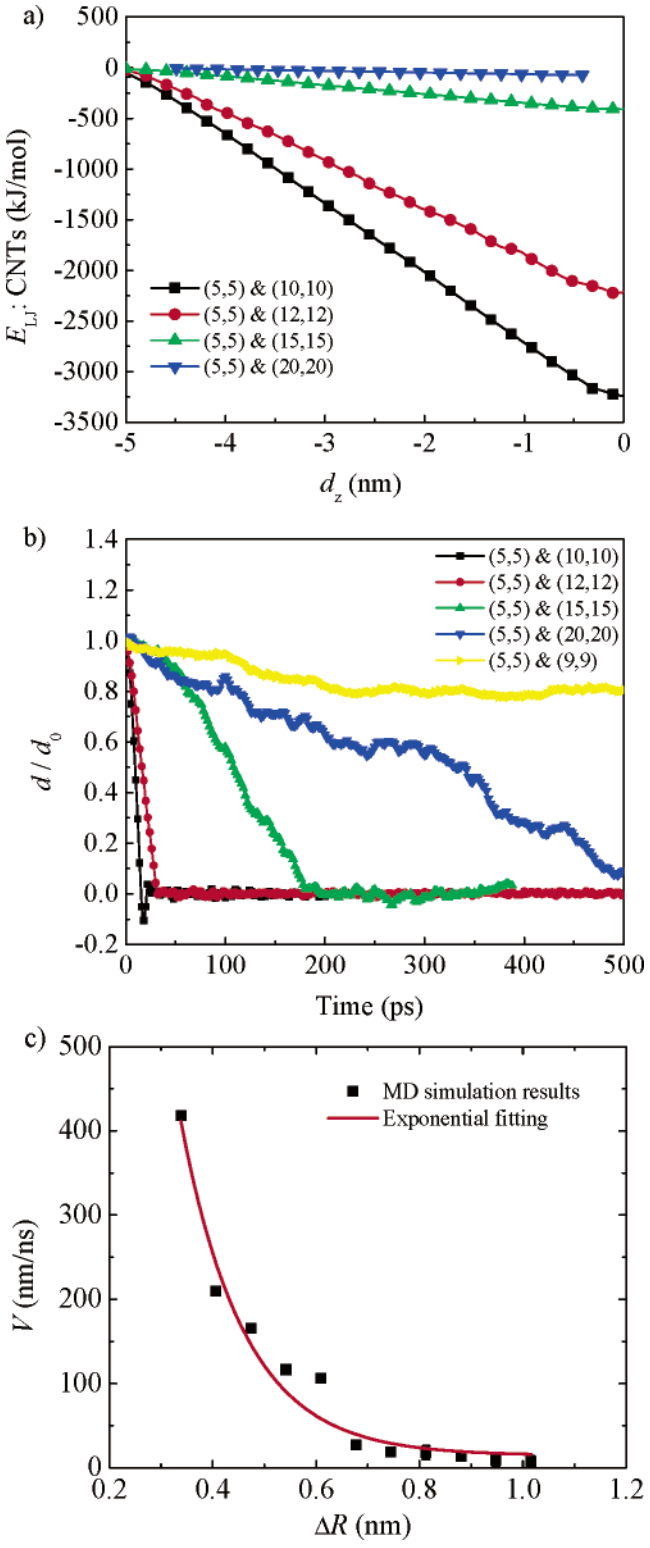

Figure 4. Size effects in CNTs assembly. (a) The evolution of the van der Waals energy between CNTs of different sizes as a function of the intertube center-of-mass (COM) distance projected in the axial direction, d_z. (b) The evolution of the normalized COM distance between CNTs as a function of time. d_0 is the initial separation between two corresponding CNTs. (c) The insertion speed as a function of the difference in radius (ΔR) of the two SWNTs.

of coaxial insertion. However, for a given small CNT, there exists a lower limit for the radius of the large CNT for successful assembly. For example, a (5,5) CNT cannot "swim" into a (9,9) (as shown by the yellow curve in Figure 4b) because the radius of the (9,9) is smaller than the lower limit. In this case $\Delta R = R_{(9,9)} - R_{(5,5)} = 0.2708$ nm is only 80% of $\sigma_{CC} = 0.3400$ nm, and therefore one will not be able to assemble a concentrically nested (5,5) and (9,9) bitube. Our simulation also shows that a forced (5,5)@(9,9) bitube disassembles into two SWNTs immediately after the constraint is removed.

Table 2. Parameters for Different Simulation Systems of Two SWNTs in Water[a]

(m,n)[b] for two SWNTs	radius of the small CNT (nm)	radius of the large CNT (nm)	ΔR[c] (nm)
(5,5) & (9,9)	0.3385	0.6093	0.2708
(5,5) & (10,10)	0.3385	0.6770	0.3385
(5,5) & (12,12)	0.3385	0.8125	0.4739
(5,5) & (15,15)	0.3385	1.0156	0.6770
(5,5) & (20,20)	0.3385	1.3541	1.0156
(5,5) & (17,0)	0.3385	0.6645	0.3260
(5,5) & (18,0)	0.3385	0.7036	0.3651
(9,0) & (18,0)	0.3518	0.7036	0.3518

[a] The length of armchair CNTs is 4.79 nm, and that for zigzag CNTs is 4.75 nm. [b] (m,n) are the commonly used notations for CNT indices. [c] ΔR denotes the difference in radius of the two SWNTs.

The role of CNT chirality on the self-assembly process is further investigated by comparing three representative combinations: two armchair CNTs (5,5) and (10,10), an armchair (5,5) and a zigzag (17,0), and two zigzag (9,0) and (18,0). In all three cases, the radii of the small and the large CNTs are about 0.34−0.35 nm and 0.68−0.70 nm, respectively. All of the CNTs have approximately the same length (4.79 and 4.75 nm for the armchair and the zigzag CNTs, respectively), as listed in Table 2. It is seen from the curves of the intertube COM distances in Figure 5 that the three assembly processes have almost the same insertion speed despite different chirality compositions. Therefore, the chirality does not play a significant role in the described assembly process.

We also examined the effects of temperature and pressure on the CNT assembly. It is found that the pressure does not have a prominent influence, but the increase in temperature can speed up the assembly process because of increased molecular mobility. The insertion speeds are about 400, 450, and 500 nm/ns at the temperatures 300, 350, and 400 K, respectively.

In summary, we have conducted molecular dynamics simulations to show that single-walled CNTs of different sizes and chiralities can coaxially self-assemble into multiwalled CNTs in water through a series of ultrafast insertion processes of smaller CNTs into larger CNTs. The intertube vdW interaction plays a dominating role and the assembly process is influenced strongly by the size differences between the small and large CNTs. For a given size of the small CNT, the radius of the large CNT should be properly chosen to ensure a successful assembly. For a successful and effective assembly process, the difference in radius of the small and large CNTs should be around 0.34 nm (0.335−0.36 nm),

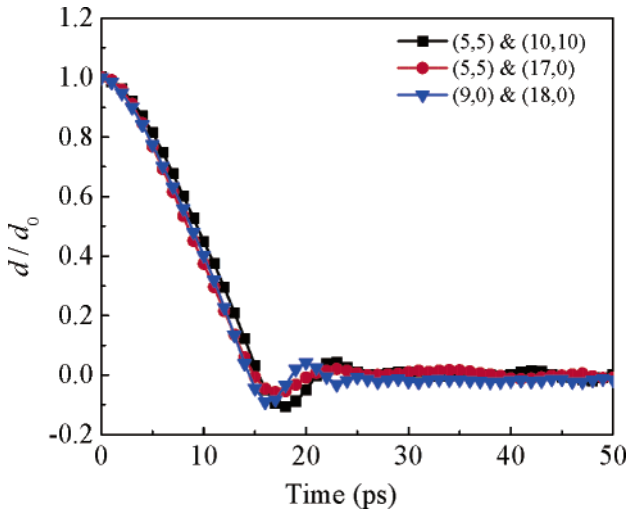

Figure 5. Chirality effect in CNT assembly. The normalized center-of-mass distance between CNTs as a function of time for systems with various chiralities. d_0 is the initial separation between two corresponding CNTs in these systems.

independent of the tube type. The increase in the radius of the large CNT will slow the assembly process and, consequently, hinder proper assembly when the radius of the large CNT becomes too large. However, the radius of the large CNT has a lower limit roughly equal to the small CNT radius plus σ_{CC}. Below this lower limit, the assembly can be totally blocked because of the repulsive short-range interactions between the two CNTs. We have not found a significant effect of the CNT chiralities on the assembly processes.

Through the stepwise shell-by-shell insertion procedure, an MWNT can be constructed from SWNTs with different lengths, diameters, and chiralities. The MWNTs formed in this way may be further developed into building blocks for novel nanoscale machines or devices,[9−16] in which the inner shells may serve as the motion-enabling axles or shafts to provide mechanical support for the outer shells as sleeves or moving parts. Another potential application for this bottom-up assembly might be in the areas of molecular nanoelectronics. For example, an MWNT assembled from SWNTs with desired chiralities (electronic properties) may have specific electronic properties and may be used to construct useful unique nanowires, capacitors, or other molecular electronic components or devices.

In addition, our results have general implications on filling nanoporous materials such as CNTs with nanoparticles (water,[26] metal,[29,30] fullerene,[31] metallofullerene[32]) or tubular structures (biomolecules[33−36] and CNTs) via the nonspecific, nonbonding vdW interactions. This vdW-driven assembly approach presents an attractive and efficient way to start from a set of given nanostructures and build them into more complex structures with targeted characteristics. The potential of such bottom-up fabrication routes is yet to be fully explored. Further theoretical study of such types of self-assembly phenomena is currently underway.

Acknowledgment. Financial support of this work was provided by NSFC (grant nos. 10525210, 10121202, 1044-2002, and 10502031), 973 Project (grant no. 2004CB619304), Fok Ying Tong Education Foundation and the Max Planck Society. In addition, J.Z. acknowledges a Visiting Ph.D. Student Fellowship at the Max Planck Institute for Metals Research during 2002−2003 and many helpful discussions with Dr. Y. Kong and Dr. Z. P. Xu. H.G. acknowledges an Oversea Young Investigator Award from NSFC and a Chang Jiang Scholarship from Tsinghua University.

References

(1) Bernholc, J.; Brenner, D.; Nardelli, M. B.; Meunier, V.; Roland, C. *Annu. Rev. Mater. Res.* **2002**, *32*, 347.
(2) Shenderova, O. A.; Zhirnov, V. V.; Brenner, D. W. *Crit. Rev. Solid State* **2002**, *27*, 227.
(3) Baughman, R. H.; Zakhidov, A. A.; de Heer, W. A. *Science* **2002**, *297*, 787.
(4) Martin, C. R.; Kohli, P. *Nat. Rev. Drug Discovery* **2003**, *2*, 29.
(5) Iijima, S. *Nature* **1991**, *354*, 56.
(6) Drexler, K. E. *Nanosystems: Molecular Machinery, Manufacturing, and Computation*; Wiley: New York, 1992.
(7) Yu, M. F.; Lourie, O.; Dyer, M. J.; Moloni, K.; Kelly, T. F.; Ruoff, R. S. *Science* **2000**, *287*, 637.
(8) Cumings, J.; Zettl, A. *Science* **2000**, *289*, 602.
(9) Tuzun, R. E.; Noid, D. W.; Sumpter, B. G. *Nanotechnology* **1995**, *6*, 64.
(10) Forro, L. *Science* **2000**, *289*, 560.
(11) Zheng, Q. S.; Jiang, Q. *Phys. Rev. Lett.* **2002**, *88*, 045503.
(12) Legoas, S. B.; Coluci, V. R.; Braga, S. F.; Coura, P. Z.; Dantas, S. O.; Galvao, D. S. *Phys. Rev. Lett.* **2003**, *90*, 055504.
(13) Fennimore, A. M.; Yuzvinsky, T. D.; Han, W. Q.; Fuhrer, M. S.; Cumings, J.; Zettl, A. *Nature* **2003**, *424*, 408.
(14) Bourlon, B.; Glattli, D. C.; Miko, C.; Forro, L.; Bachtold, A. *Nano Lett.* **2004**, *4*, 709.
(15) Han, J.; Globus, A.; Jaffe, R.; Deardorff, G. *Nanotechnology* **1997**, *8*, 95.
(16) Kang, J. W.; Hwang, H. J. *Nanotechnology* **2004**, *15*, 1633.
(17) Meyer, J. C.; Paillet, M.; Roth, S. *Science* **2005**, *309*, 1539.
(18) Stellacci, F. *Nat. Mater.* **2005**, *4*, 113.
(19) Walther, J. H.; Jaffe, R.; Halicioglu, T.; Koumoutsakos, P. *J. Phys. Chem. B* **2001**, *105*, 9980.
(20) Lindahl, E.; Hess, B.; van der Spoel, D. *J. Mol. Mod.* **2001**, *7*, 306.
(21) van der Spoel, D.; Lindahl, E.; Hess, B.; van Buuren, A. R.; Apol, E.; Meulenhoff, P. J.; Tieleman, D. P.; Sijbers, A. L. T. M.; Feenstra, K. A.; van Drunen, R.; Berendsen, H. J. C. *Gromacs User Manual*, version 3.2; Groningen: Netherlands.
(22) Berendsen, H. J. C.; Postma, J. P. M.; van Gunsteren, W. F.; DiNola, A.; Haak, J. R. *J. Chem. Phys.* **1984**, *81*, 3684.
(23) Jorgensen, W. L.; Chandrasekhar, J.; Madura, J. D.; Impey, R. W.; Klein, M. L. *J. Chem. Phys.* **1983**, *79*, 926.
(24) Darden, T.; York, D.; Pedersen, L. *J. Chem. Phys.* **1993**, *98*, 10089.
(25) Essmann, U.; Perera, L.; Berkowitz, M. L.; Darden, T.; Lee, H.; Pedersen, L. G. *J. Chem. Phys.* **1995**, *103*, 8577.
(26) Hummer, G.; Rasaiah, J. C.; Noworyta, J. P. *Nature* **2001**, *414*, 188.
(27) Wallqvist, A.; Gallicchio, E.; Levy, R. M. *J. Phys. Chem. B* **2001**, *105*, 6745.
(28) Beckstein, O.; Biggin, P. C.; Sansom, M. S. P. *J. Phys. Chem. B* **2001**, *105*, 12902.
(29) Ajayan, P. M.; Iijima, S. *Nature* **1993**, *361*, 333.
(30) Dujardin, E.; Ebbesen, T. W.; Hiura, H.; Tanigaki, K. *Science* **1994**, *265*, 1850.
(31) Smith, B. W.; Monthioux, M.; Luzzi, D. E. *Nature* **1998**, *396*, 323.
(32) Hirahara, K.; Suenaga, K.; Bandow, S.; Kato, H.; Okazaki, T.; Shinohara, H.; Iijima, S. *Phys. Rev. Lett.* **2000**, *85*, 5384.
(33) Gao, H.; Kong, Y.; Cui, D.; Ozkan, C. S. *Nano Lett.* **2003**, *3*, 471.
(34) Gao, H.; Kong, Y. *Annu. Rev. Mater. Res.* **2004**, *34*, 123.
(35) Ito, T.; Sun, L.; Crooks, R. M. *Chem. Commun.* **2003**, 1482.
(36) Yeh, I. C.; Hummer, G. *Proc. Natl. Acad. Sci. U.S.A.* **2004**, *101*, 12177.

NL052289U